ARCTIC
VOL. 45, NO. 3 (SEPTEMBER 1992) P. 258-268

# A Description of Summer Physical Oceanographic Conditions in Rupert Bay (James Bay, Canada)[1]

L. VEILLEUX,[2] R.G. INGRAM[2] and A. VAN DER BAAREN[2]

*(Received 28 May 1991; accepted in revised form 5 December 1991)*

ABSTRACT. Measurements of current velocity, temperature, salinity, and water level were made over a period of two months in Rupert Bay, James Bay (Canada). From an analysis of the current meter time series, the circulation and distribution of physical properties were found to be dominated by the tides, with the semi-diurnal component being the predominant component. An analysis of variance revealed that 77% of the salinity variations were related to the tides. Vertically homogeneous conditions prevailed in many areas because of a large tidal amplitude/depth ratio of 0.625, causing intense mixing in two-thirds of the estuary. Non-tidal velocity components were found to be O(1) less than tidal currents, with the long-term mean circulation directed out of the bay. Non-tidal water level variations were well correlated with the wind. The maximum cross-correlation coefficient was calculated to be 0.77 for a 7 hour lag. The centrifugal force, Coriolis force, and baroclinic pressure gradient were dominant forces driving the secondary flows of the bay. Tidal fronts were found to be either aligned parallel to the main axes of principal channels or around small downstream islands with the arrangement influenced by bottom topography.

Key words: estuary, circulation, tides, salinity, mixing, secondary flow, front

RÉSUMÉ. Des données de vitesse de courant, de température, de salinité et de niveau d'eau furent échantillonnées pendant une période de deux mois dans la Baie de Rupert, Baie James (Canada). Suite à l'analyse des séries chronologiques alors obtenues, il apperait que la circulation et la répartition des propriétés physiques étaient déterminées par les marées et que la constituante semi-diurne y dominait toute autre constituante de la marée. Une analyse de variance a révélé que 77% des variations de la salinité étaient attribuables aux marées semi-diurne. L'homogénéité de la colonne d'eau observée en plusieurs endroits semblait liée au fort rapport amplitude/profondeur (0,625) qui favoriserait un intense phénomène de mélange pour les deux tiers de l'estuaire. Les composantes de la vitesse étaient O(1) moins que les courants de marée. La circulation à long terme étaient dans la direction avale. Les variations de niveau d'eau non expliquées par la marée étaient apparemment induites par le vent; le coefficient de correlation croisée maximum calculé ont été de 0.77 pour un déphasage de 7 heures. Les fronts de marées observés soit étaient parallèles à les axes principaux des chenaux principaux ou suivaient le contour des petites îles sises en aval à l'entrée de la baie. L'arrangement de ces fronts semblait être influencé par la topographie du fond marin.

Mot clés: estuaire, circulation, marées, salinité, mélange, courant secondaire, front

## INTRODUCTION

Since the early 1970s, extensive oceanographic field studies have been undertaken in the coastal areas of southeastern Hudson Bay and eastern James Bay. The renewed interest in a region that had been neglected for so many years (Dunbar, 1982) arose because of plans to develop major hydroelectric projects on many rivers in northern Quebec.

In 1982, Prinsenberg published a paper predicting effects of hydroelectric development on river discharge and, ultimately, on the circulation of James Bay (Prinsenberg, 1982; see also Prinsenberg, 1980, for effects on other sites in Hudson Bay.) He used an estuarine circulation model and considered the salt balance of the system for both summer and winter conditions. His model predicted increased discharge in winter and a doubling of the near-surface coastal currents in the bay. Prinsenberg's model was taken from earlier studies of the relationship between circulation and salt flux (in which similarity solutions were obtained for pairs of partial differential equations). Hansen and Rattray (1965), Kjerfve (1986), and Pritchard (1967) provide detailed discussions of salt balance and gravitational circulation in estuaries. Rather than provide an inventory of the work that has dealt with physical processes in estuaries, we refer the reader to two comprehensive volumes by Dyer (1973) and Officer (1976), in which they have explained the physical oceanography of estuaries and have given examples of theory applied to many estuaries in the world.

The data analyzed in the present study were collected during the summer of 1976 by the Groupe Inter-universitaire de Récherches Océanographiques du Québec (GIROQ) under contract with the Société d'Énergie de la Baie James (SEBJ). Measurements of current velocity, temperature, salinity, and water level were made over a period of two months in Rupert Bay, which is a large, shallow estuary located in the southeastern corner of James Bay. The goal was to gather information on the physical oceanography, the sedimentological regime, and the biological oceanography (including benthos and fish, as well as the ecology of the coastal marshes) of Rupert Bay. The results of those observations were reported in a number of technical reports and a few articles (Legendre and Simard, 1978; d'Anglejan, 1980; Ingram and Chu, 1987).

The objectives of this paper are to describe the summer physical oceanographic characteristics in Rupert Bay and to understand some of the variability on the basis of tidal, meteorological, and freshwater forcing. We begin with a general description of the study area and follow with a brief description of sampling and analysis of the current meter time series. Main features of the circulation and mixing patterns were obtained from the time series analysis, and these results are discussed in several sections detailing the salinity distribution, tidal regime, circulation, and frontal regime in Rupert Bay.

## THE STUDY AREA — RUPERT BAY

Rupert Bay is a very large, shallow, subarctic estuary located off the southeast corner of James Bay (Fig. 1) in the physiographic region of the Eastmain Lowland. Its dimensions are approximately 60 km long by 20 km wide and it covers an area of about 875 km$^2$. The estuary is characterized by large

[1]Contribution to the program of GIROQ (Groupe inter-universitaire de recherche océanographiques du Québec)
[2]Department of Meteorology, McGill University, 805 Sherbrooke Street West, Montreal, Quebec, Canada H3A 2K6

seasonal fluctuations in river runoff (annual peak discharge in May) and by alternation between an ice-covered and an open-water period, both approximately six months in duration. Rupert Bay receives a mean annual freshwater discharge of about 2340 $m^3 \cdot s^{-1}$ from four rivers: the Nottaway (1020 $m^3 \cdot s^{-1}$), Broadback (320 $m^3 \cdot s^{-1}$), Rupert (870 $m^3 \cdot s^{-1}$), and Pontax (130 $m^3 \cdot s^{-1}$). Low water depths of 3-5 m characterize most of the study region. Downstream of Stag Rock, three deeper channels extending inland from James Bay can be found: Inenew, Emelia, and Boat passages. Maximum channel depths are less than 15 m.

The bottom of Rupert Bay is covered by silts and clays of Tyrrell Sea deposits, which provide an abundant source of fine sediments and make the waters very turbid in summer (d'Anglejan, 1980). The shoreline is marked by large marshes and muddy foreshores, particularly in Cabbage Willows Bay and between the mouths of the Broadback and Rupert rivers.

The estuary has an important phytoplankton production in the downstream region, while the relative abundance and diversity of fish species are quite high (Legendre and Simard, 1978).

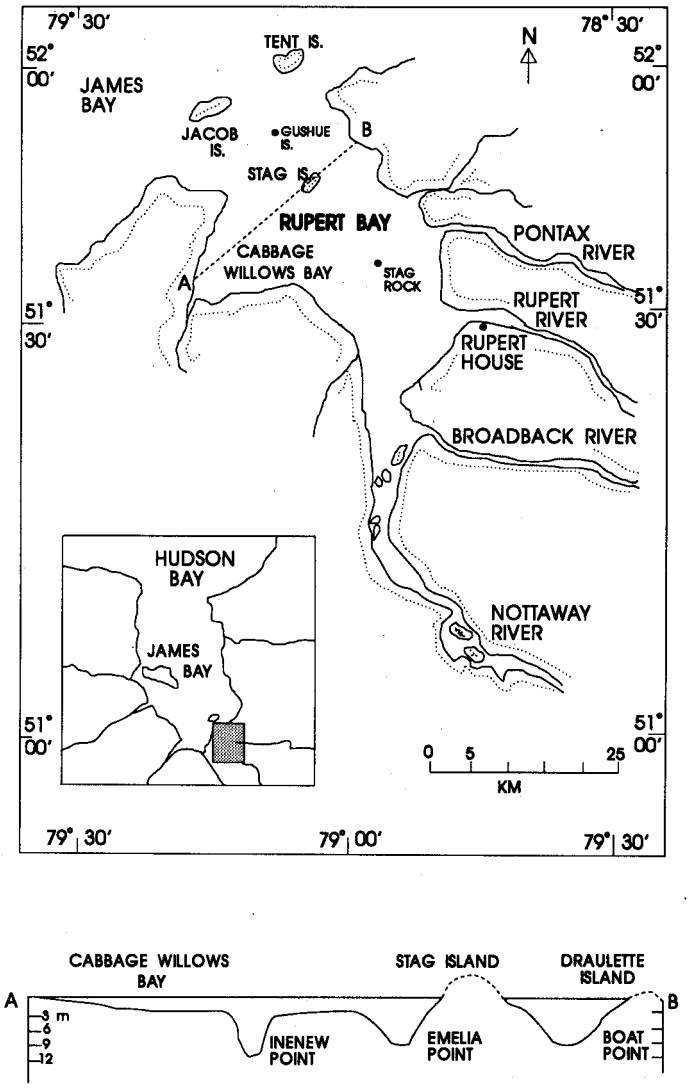


FIG. 1. Location of Rupert Bay and cross-channel bathymetric profile showing main passages.

## METHODOLOGY

During a 45-day program in July and August 1976, and for a short time in late summer of the same year, Aanderaa RCM-4 current meters were moored at different locations within the bay to monitor current speed and direction, temperature, and conductivity (salinity) with a 5 min sampling interval. Further temperature and conductivity measurements were taken with a Martek TDC profiler at 62 stations, 13 of which were measured over a period of 12.5 h from anchored sites within the bay. A limited number of observations were also taken in late summer after the main work was completed.

An Aanderaa water level recorder was moored near the entrance of the bay (station 9) for a 33-day period, during which time the instrument moved slightly.

A meteorological station (air temperature, wind speed, and direction) was positioned on Gushue Island from 19 July to 19 August at 38 m above sea level. Other meteorological data for Moosonee (100 km west of Rupert Bay) were obtained from the Atmospheric Environment Service. Bathymetric features of the estuary were taken from the Canadian Hydrographic Service map number 5414, and daily freshwater runoff values for the three main tributaries were provided by the Ministère de l'Environnement du Québec.

Figure 2 shows the mooring and anchored sites, the position of the meteorological station, and the position of the water level recorder. Figure 3 shows a time line of when the moored instruments were in place and when the anchored sites were sampled.

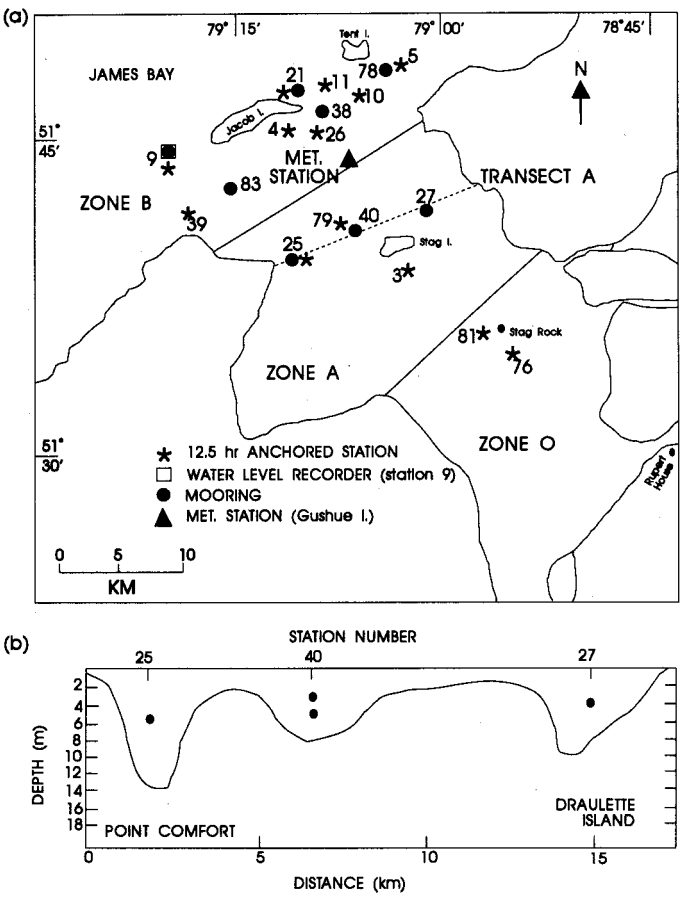


FIG. 2. a) Sampling scheme and primary zone designation. b) Bathymetric profile of transect A and mooring scheme.

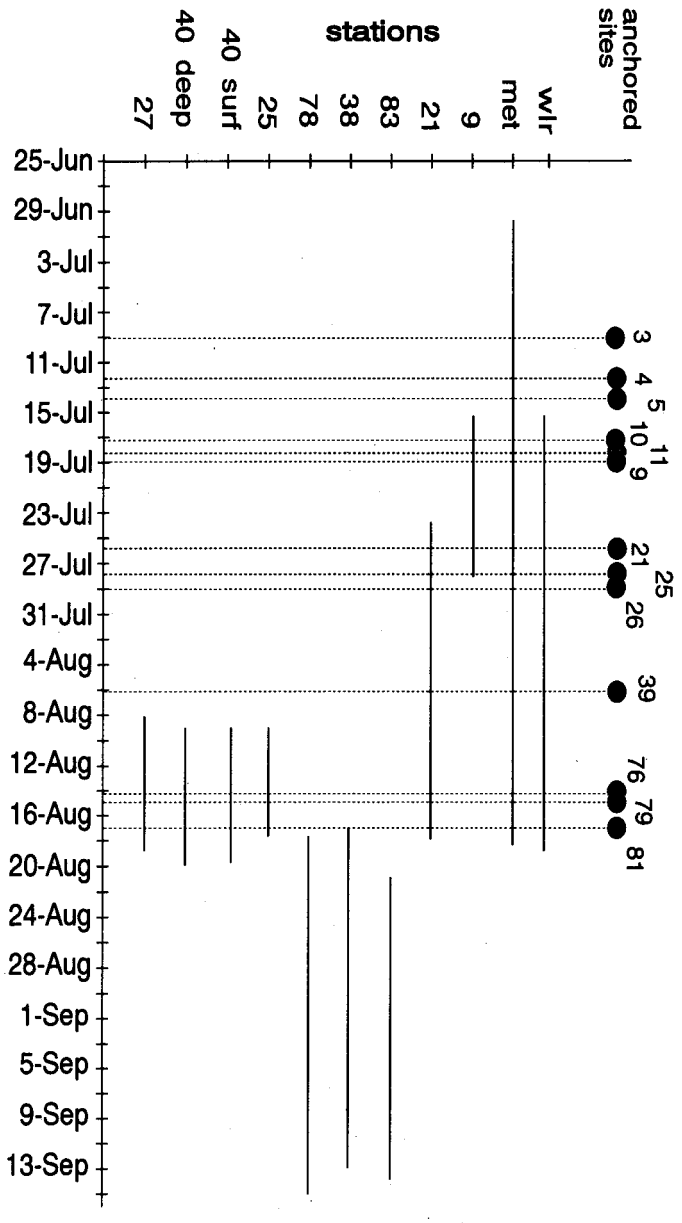


FIG. 3. Time line showing sampling times of moorings, anchored sites, meteorological station (met), and water level recorder (wlr).

All current and wind vectors were decomposed into along-channel components (u), positive into the bay (135° true), and cross-channel components (v), positive along 45° true. It is anticipated that some contamination of the velocity data occurred because of wave-induced motions in the savonius rotors for the near-surface moorings. Current meter data were filtered using an $A_6A_6A_7/6^*6^*7$ type moving mean to reduce the relative frequency of observations to hourly values. Smoothed hourly values were also filtered with an $A_{24}A_{24}A_{25}/24^*24^*25$ filter to eliminate diurnal and higher frequencies, according to the methods discussed in Godin (1972). A complete description of the equipment and methods is given in Veilleux (1990).

## RESULTS AND DISCUSSION

Table 1 gives a summary of the mean temperatures, salinities, and mean and root mean square (rms) current velocities (along-channel only) over the sampling period. To help in understanding the important mixing processes and driving forces, a variance analysis was performed on the unfiltered, smoothed, and low-pass filtered salinity time series. Figure 4 shows the results of the analysis as well as the percentage of the salinity variance due to high frequency events, semi-diurnal and diurnal tidal frequencies, and low frequency events. It was found that 77% of the salinity variations in Rupert Bay were related to tidal phenomena (semi-diurnal and diurnal components), 12% to other high-frequency events (assumed to be mostly related to winds), and 11% to low frequencies (atmospheric systems, long period tidal components, river runoff, etc.).

### *Salinity Distribution*

The upper limit of the salt intrusion at high tide was located near Stag Rock, while at full ebb, fresh water could be found as far downstream as Stag Island. Figure 5 illustrates the isohaline distribution at the surface and at 5 m, for both the ebb tide (L±1) and the flood tide (H±1). The data used for this figure were from all the CTD stations sampled in a 2 h period centred at low and high tides. These samples were taken on various days during the 45-day study period with no pre-determined regularity. The figure is not a synoptic representation due to the variability of tidal currents, winds, James Bay salinities, and freshwater input during that period. Significant stratification is found only at H+1 in the area near Stag Island. We

TABLE 1. RCM moorings — number of days of sampling, depth of instrument, mean and rms ($U$) current velocities, mean temperature, and mean salinity

| Station | No. of days | Depth of instr. (m) | $\bar{u}$ (cm·s$^{-1}$) | $\bar{v}$ (cm·s$^{-1}$) | $U$ (cm·s$^{-1}$) | $\bar{T}$ (°C) | $\bar{S}$ (ppt) |
|---|---|---|---|---|---|---|---|
| Zone B | | | | | | | |
| 9 | 13 | 4 | –7 | –4 | 51 | 11.9 | 11.0 |
| 21 | 25 | 10 | 5 | 9 | 63 | 9.9 | 15.0 |
| 83* | 25 | 4 | –8 | –1 | 41 | 11.5 | 13.3 |
| 38 | 31 | 5 | –4 | 16 | 42 | 13.2 | 11.8 |
| 78 | 27 | 11 | 3 | –12 | 25 | 11.1 | 14.9 |
| Zone A | | | | | | | |
| 25 | 9 | 3 | –6 | –12 | 78 | 6.7 | 14.1 |
| 40 | 11 | 4 | –7 | –3 | 46 | 12.9 | 9.7 |
| 40 | 11 | 8 | 0 | –10 | 28 | 9.8 | 12.9 |
| 27 | 10 | 3 | –5 | –11 | 56 | 13.4 | 8.8 |

*Station 83: mooring moved during sampling period.

also see that the major part of the intrusion is in the area around Jacob Island.

The change in stratification along the bay is well represented in Figure 6, which shows salinity contours for three CTD stations just outside Rupert Bay and for one CTD station between Stag and Gushue islands (meteorological station location in Fig. 2). The time period for the plots is equivalent to a semi-diurnal tidal period, with slack water occurring at approximately H+2 and L+2, and maximum ebb and flood current velocities being reached 1-2 h before tidal extrema. The currents superimposed on the contours are taken from moorings located at the same stations. To illustrate the tremendous effect of the tides, it is interesting to note that except at slack high water, at station 79 (Fig. 6d) the water remained in an essentially homogeneous state and maintained this homogeneity throughout the 8 m depth as the salinity increased by 10 ppt during the course of the flood tide. Station 9 was located near the more southern boundary of James Bay and Rupert Bay. We can see that at this station the water was well stratified and that salinity reached its maximum soon after high water and its minimum just after low water. The freshest water appeared at low water but was confined to the upper 5 m. This is in accordance with Figure 5. Station 21 also showed definite stratification, although the effects of maximum ebb and flood tides are more pronounced here. Velocities at station 5 were over 150 $cm \cdot s^{-1}$ during the ebb tide. Channel orientation is responsible for the 90° difference between the direction of the velocity component at this station and the other stations. Salinities throughout the water column at station 5 were lower relative to the other two stations at the boundary of James Bay and Rupert Bay. At low water, the fresher water reached greater depths than at station 9. We infer that the majority of the fresh water exits Rupert Bay between Tent Island and the mainland.

For reference purposes, we have divided Rupert Bay into three zones according to prevalent salinity characteristics (Fig. 2). Similar zonal designations were employed by Legendre and Simard (1978) in their phytoplankton study of the region. Zone O is the area farthest upstream, where fresh water was present at all times and depths. The middle estuary, zone A, is where salinity profiles showed essentially vertically homogeneous conditions but for the duration of the ebb tide and at H+1. Zone B is found farthest downstream, and it is here that partially mixed conditions prevailed, especially in the passages around Jacob and Tent islands. The boundaries of these zones are transient and will change depending on discharge and tidal strength, as in the case of the extent of salt intrusion mentioned earlier.

### *Tidal Regime*

The predominance of the semi-diurnal components of the tide can be seen in the tidal height analysis results and in the current meter observations. Table 2 gives the amplitude and Greenwich phase lag for the principal tidal constituents that were obtained from the tide gauge data (Foreman, 1977). Table 3 lists results from a tidal current analysis (Foreman, 1978). In both tables, the constituent, $Z_0$, represents the average water level or amplitude at 0 frequency (see Forrester, 1983, for a concise explanation of tidal analysis). Both analyses reveal a strong $M_2$ tide. The tidal ellipses for the principal lunar constituent ($M_2$) are shown in Figure 7. The diurnal component is

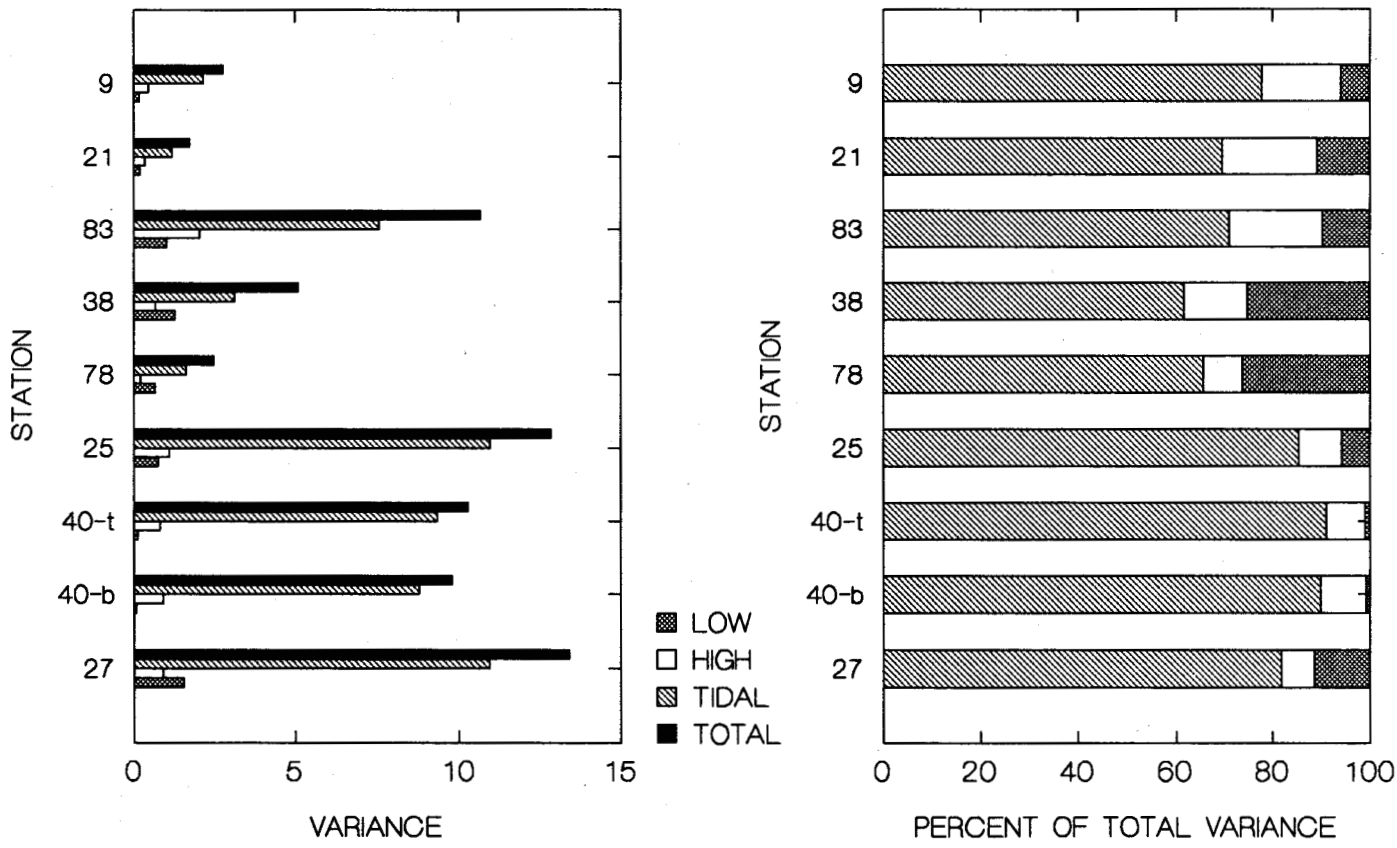


FIG. 4. Variance analysis of recorded salinities. 40-t represents the surface instrument at station 40 and 40-b represents the deeper instrument at that station. Note that the mooring at station 83 was moved during the sampling period.

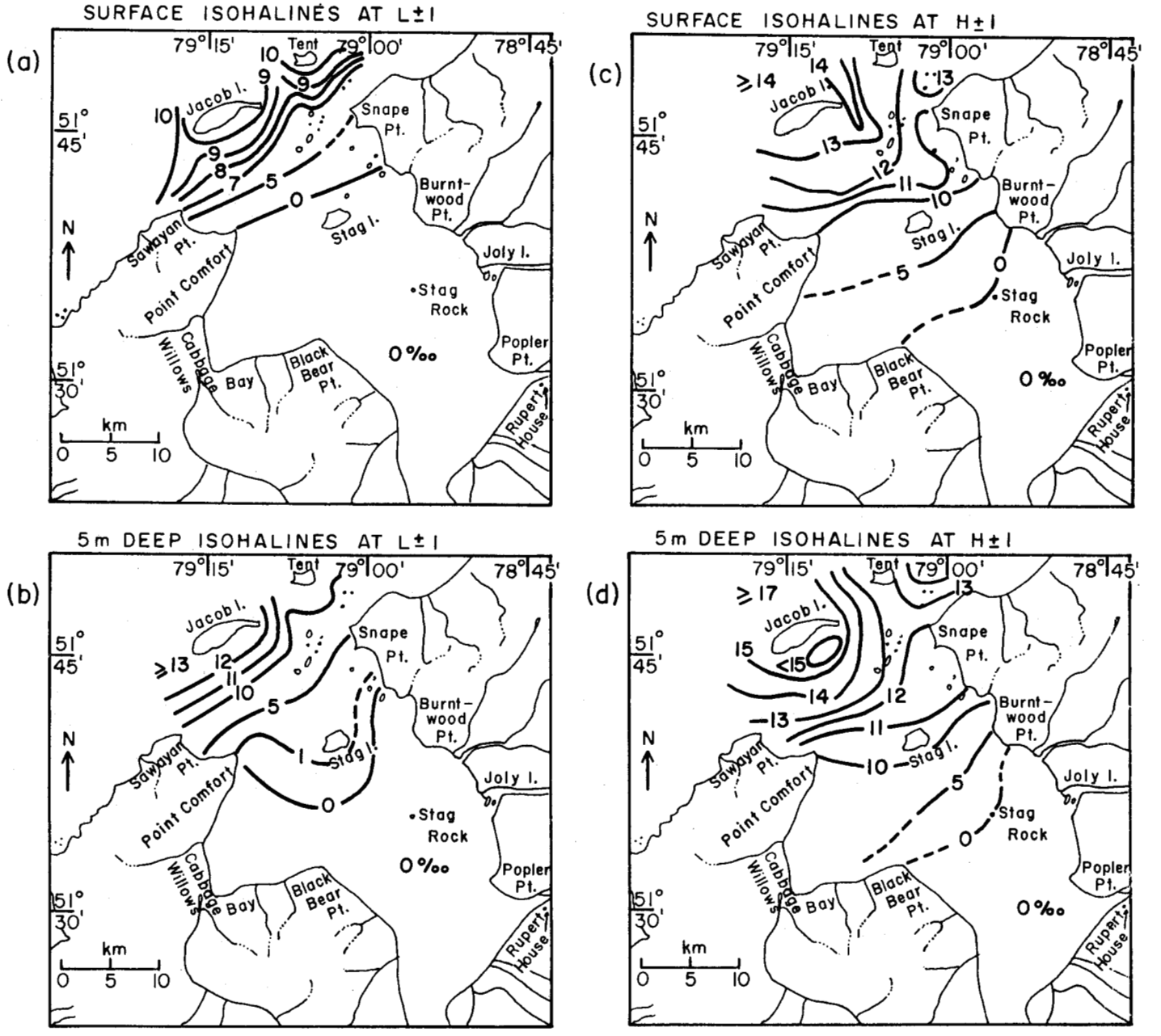


FIG. 5. Isohalines at surface and at 5 m for: a) and b) ebb tide (L±1), and for: c) and d) flood tide (H±1).

almost equivalent in amplitude to the semi-diurnal $S_2$ component. The water level signal could have been influenced by the land-sea breeze (T ≈ 24 h), which was observed on 22 of the 43 days of the sampling period (Veilleux, 1990). The quarter-diurnal component ($M_4$, T = 6.21 h), which appeared significant in both analyses, could have included a seiche effect. The seiche period for Rupert Bay ranges between 6.1 and 7.1 h and is close enough to the $M_4$ tidal period for resonance to increase the amplitude. The occurrence and strength of both the seiche effect and the land-sea breeze are unpredictable; nevertheless, the importance of wind-generated phenomena at periods close to the tidal constituents should be considered.

Estimation of the tidal form number (Defant, 1960), which is defined as the ratio (F) of the main semi-diurnal ($M_2$+$S_2$) to the main diurnal ($K_1$+$O_1$) constituent amplitudes, also confirmed the strong semi-diurnal character of the tide. A form number greater than 3 indicates that the tide is of diurnal type, and one smaller than 0.25 is considered to represent a semi-diurnal tide. Table 4 presents form numbers within the study area for both currents ($F_c$) and water level ($F_w$). For those moorings with less than 15 days of recorded data, $S_2$ and $O_1$ components were assumed to be included in the $M_2$ and $K_1$ estimations respectively. The average value of $F_c$ computed from tidal currents was 0.10. The value of $F_w$ computed from the water level recorder data was 0.24. These results fit the observations of semi-diurnal tidal currents in the inlets of Mississippi Sound (Seim and Sneed, 1988), with $F_c \approx F_w/2$. Seim and Sneed (1988) explained that continuity considerations cause semi-diurnal currents to increase relative to diurnal currents at inlets, while water levels are not affected by the continuity constraint. There are no comparable data in this study for the offshore tides, but the spatial distribution of $F_c$ from Table 4 reveals a progression from maximum values at the entrance of the bay to minimum values at inshore stations.

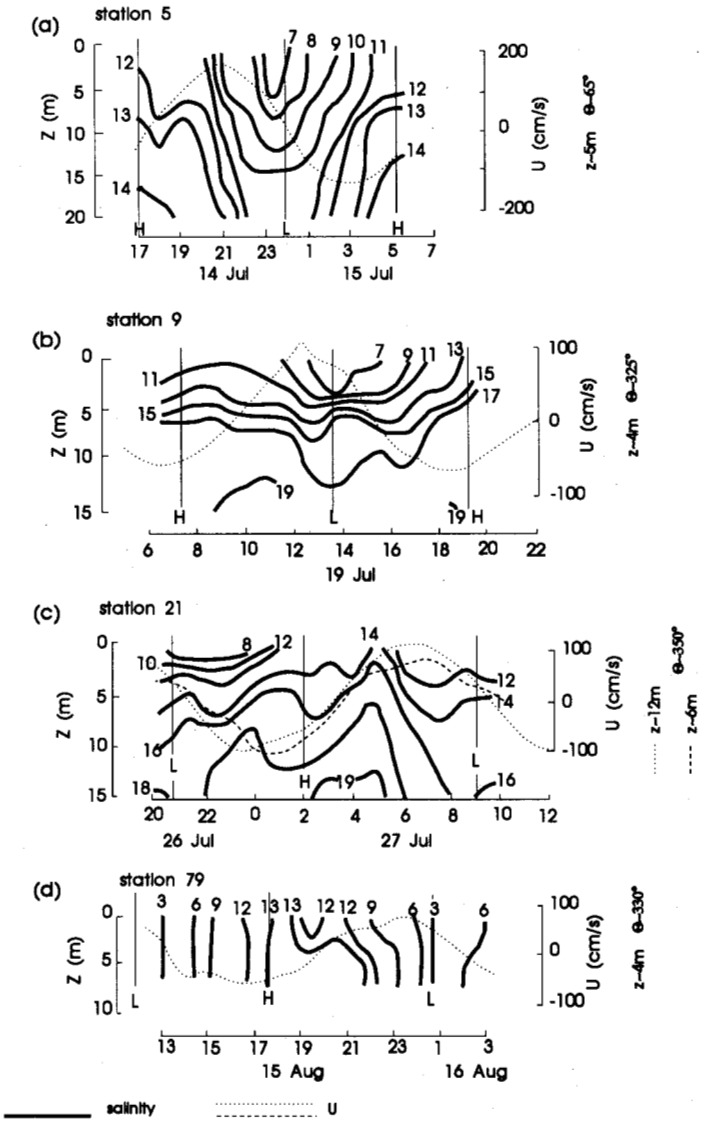


FIG. 6. Salinity contours for four stations in Rupert Bay, three just outside the bay in the stratified zone (a, b, and c), and one in the well-mixed zone inside the bay.

Calculation of the $M_4/M_2$ ratio, often called the shallow water effect ratio, gives an indication of the degree of non-linear response of the estuary to tidal forcing. This non-linearity in the tides can be illustrated by comparing offshore tides with the estuary tide. In Rupert Bay, this ratio had a value of 0.10 at the water level recorder station. We do not have offshore tide values outside Rupert Bay, but Aubrey and Speer (1985) estimated a shallow water effect ratio of 0.007 for a station outside a narrow, shallow estuary with the ratio equivalent to 0.265 within the estuary.

A comparison of the predicted tide in Rupert Bay for the period of the study with the observed water level signal allowed us to estimate the non-tidal response in the bay. A record length of 33 days is barely adequate for doing this estimation. Non-tidal forcing within the bay includes large-scale atmospheric effects, local wind driving, and seiches (resonance within the bay). Inverse barometric effects were removed from the water level signal. The resulting filtered signal of the water level, within which the fortnightly modulation can be seen, was significantly perturbed by the wind (Fig. 8). The dominant wind direction is along the main axis of the bay (from James

TABLE 2. Analysis of hourly tidal heights for station 9 from 0600, 16 July 1976 to 1700, 18 August 1976

| Name | Frequency (cycle·day$^{-1}$) | Amplitude (m) | Greenwich phase lag |
|---|---|---|---|
| $Z_0$ | 0.0000 | 16.1204 | 0 |
| $MS_f$ | 0.0677 | 0.0264 | 123 |
| $O_1$ | 0.9295 | 0.0586 | 102 |
| $K_1$ | 1.0027 | 0.1702 | 155 |
| $N_2$ | 1.8960 | 0.0963 | 23 |
| $M_2$ | 1.9323 | 0.7538 | 63 |
| $S_2$ | 2.0000 | 0.1761 | 158 |
| $M_3$ | 2.8984 | 0.0049 | 233 |
| $MN_4$ | 3.7283 | 0.0099 | 322 |
| $M_4$ | 3.8645 | 0.0717 | 351 |
| $S_4$ | 4.0000 | 0.0074 | 135 |
| $2MK_5$ | 4.8673 | 0.0028 | 147 |
| $M_6$ | 5.7968 | 0.0155 | 152 |
| $M_8$ | 7.7291 | 0.0035 | 139 |

TABLE 3. Final analysis results in current ellipse form for station 27 from 1900, 8 August 1976 to 0700, 18 August 1976, where inclination refers to a rotation from the positive x-axis directed to the east, and "major" and "minor" refer to the magnitudes and directions of the major and minor axes of the tidal ellipses

| Name | Frequency (cycle·day$^{-1}$) | Major axis (cm·s$^{-1}$) | Minor axis (cm·s$^{-1}$) | Inclination |
|---|---|---|---|---|
| $Z_0$ | 0.0000 | 12.4 | 0.0 | 23 |
| $K_1$ | 1.0032 | 6.0 | 1.1 | 136 |
| $M_2$ | 1.9323 | 73.7 | 3.5 | 123 |
| $M_3$ | 2.8984 | 1.9 | 0.6 | 68 |
| $M_4$ | 3.8645 | 7.4 | –3.3 | 37 |
| $2MK_5$ | 4.8673 | 2.9 | 1.7 | 48 |
| $2SK_5$ | 5.0027 | 3.2 | –0.2 | 113 |
| $M_6$ | 5.7968 | 10.2 | 2.2 | 82 |
| $3MK_7$ | 6.7996 | 2.3 | 1.0 | 89 |
| $M_8$ | 7.7291 | 2.7 | 0.3 | 47 |

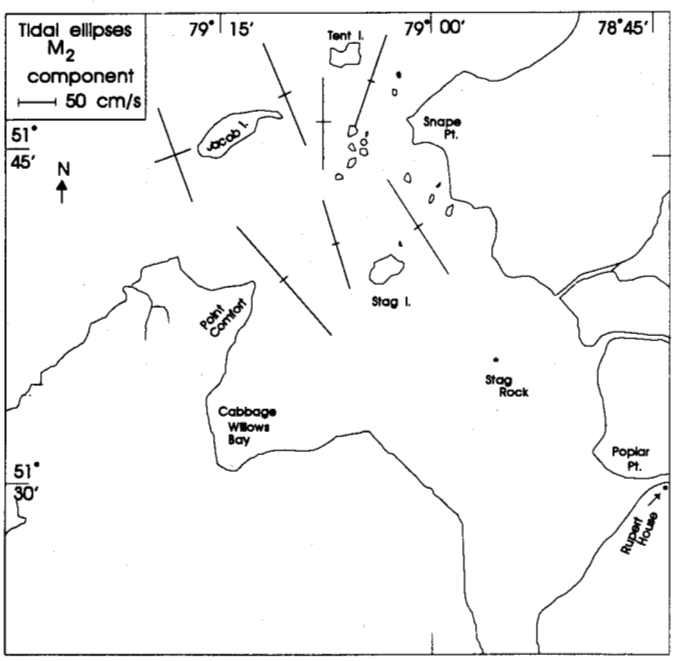


FIG. 7. Tidal ellipses for $M_2$ tidal currents in Rupert Bay.

Bay). Figure 8 shows that the wind was an important disturbing factor for the water level signal. A lagged cross-correlation analysis of the two time series gave a maximum correlation coefficient (r) of 0.77, with a 7 h lag due mainly to the sea-level setup time in response to an imposed wind.

TABLE 4. Tidal current analysis: F is the tidal form number[1] ($F_c$ for the tidal current and *Fw* for the tide gauge), and $M_4/M_2$ is the shallow water effect ratio[2]

| Station | Station depth, h (m) | Instru. depth, z (m) | $F_c$ | $M_4/M_2$ |
|---|---|---|---|---|
| Zone B | | | | |
| 9* | 17 | 4 | 0.12 | 0.13 |
| 21 | 14 | 10 | 0.10 | 0.06 |
| 83 | 9 | 4 | 0.16 | 0.14 |
| 38 | 13 | 5 | 0.04 | 0.14 |
| 78 | 12 | 11 | 0.10 | 0.08 |
| Zone A | | | | |
| 25* | 12 | 3 | 0.06 | 0.10 |
| 40* | 8 | 4 | 0.09 | 0.04 |
| 40* | 8 | 8 | 0.12 | 0.14 |
| 27* | 8 | 3 | 0.08 | 0.10 |

[1]Tidal form number for the tide gauge: $F_w = 0.24$.
[2]Shallow water effect ratio for the tide gauge: $M_4/M_2 = 0.10$.
*Mooring period less than 15 days.

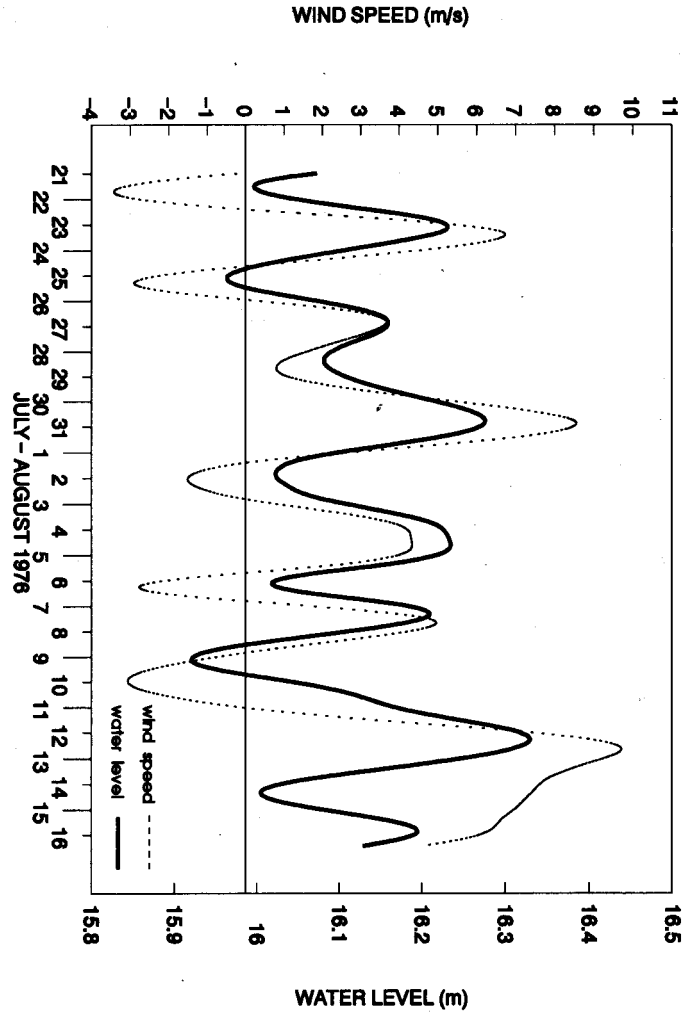


FIG. 8. Comparison of the U velocity component of the wind (recorded on Gushue Island) with the filtered water level signal.

*Circulation*

Current meter data, decimated to hourly intervals, from stations 25, 40, and 27 (transect A in Figure 2) are shown in Figure 9. One can clearly see the semi-diurnal variability in the four time series. At station 40, the temperature and salinity fields are similar at both depths because of near homogeneity of the water column in this area (Figs. 9b and 9c). With reference to the velocity, however, magnitudes are much less at 8 m than at 4 m due to a bottom depth of only 10 m. Also at station 40, during maximum ebb tide, large negative values were observed in the cross-channel velocity (v) at times when the current appeared weak in the along-channel (u) component. Several rapid changes to negative v values occurred in the middle of positive u peaks. These shifts were associated with passing fronts. At station 25, v was virtually equivalent in magnitude at all times to u, and at station 27, v was equivalent to u in strength during the flood tide.

All available current meter data from all the moorings and fixed stations were combined to give a picture of the tidal circulation shown in Figure 10. The data for these two plots were not all sampled on the same day and there was no accounting for a variable tidal amplitude. The figure shows the ebb and flood currents at 3 m depth. The data are plotted for the time of maximal ebb flow (5 h after high water) and for the time of maximum flood (4 h after low water). We see that the strengths of the flood and the ebb were of similar magnitude, 100 $cm \cdot s^{-1}$, but the flows used different paths for flood and ebb in some shallow areas. Table 1 shows that the magnitudes of the mean velocity components were about 10% of that of the tidal flow. The long-term mean also seemed to be directed downstream. Stations 21 and 78 exhibited strong inward flow at 10 m or greater.

In estuaries with a large ratio, $\Sigma$, of tidal range to mean water depth (Rupert Bay: $\Sigma = 0.625$), local depth changes appreciably over a tidal cycle and the bottom effect on current magnitude and direction is important in shallow areas (Kjerfve, 1975). This bottom effect is due to the frictional stresses arising from bottom drag. The major disturbing influence on non-tidal mean circulation is believed to be the wind and bottom friction.

Gravitational circulation in an estuary such as Rupert Bay consists of a seaward flow of brackish water originating as river discharge, a compensating landward flow of seawater at depth, and vertical exchange between the two waters from which arises a vertical salinity gradient whose constancy is determined by the effectiveness of the exchange process. The circulation, however, is not laterally homogeneous ". . . as the water tends to flow in a spiral fashion. The transverse and vertical components of the flow create what are known as secondary flows in the plane of the cross-section" (Dyer, 1977). These flows are consequences of variations in bottom topography.

Variations of the lateral motion were examined for a cross-section of Rupert Bay (transect A in Figure 2). The equation representing the lateral balance is:

$$\bar{v}\left(\frac{\partial \bar{v}}{\partial y}\right) = -\frac{\overline{1}}{\rho}\left(\frac{\overline{\partial P}}{\partial y}\right) - f\bar{u} - \left(\frac{\overline{u^2} + \overline{U^2}}{R}\right) + \left(\frac{1}{\rho}\frac{\partial F}{\partial z}\right)$$

The local acceleration is balanced by: the pressure gradient; the effect of the Coriolis force ($f = 0.729 \times 10^{-4} \sin\phi$; $\phi$ = latitude); the centrifugal force arising from the curvature of the streamlines (R = 24 km is the radius of curvature of streamlines estimated from aerial photographs and U is the tidal

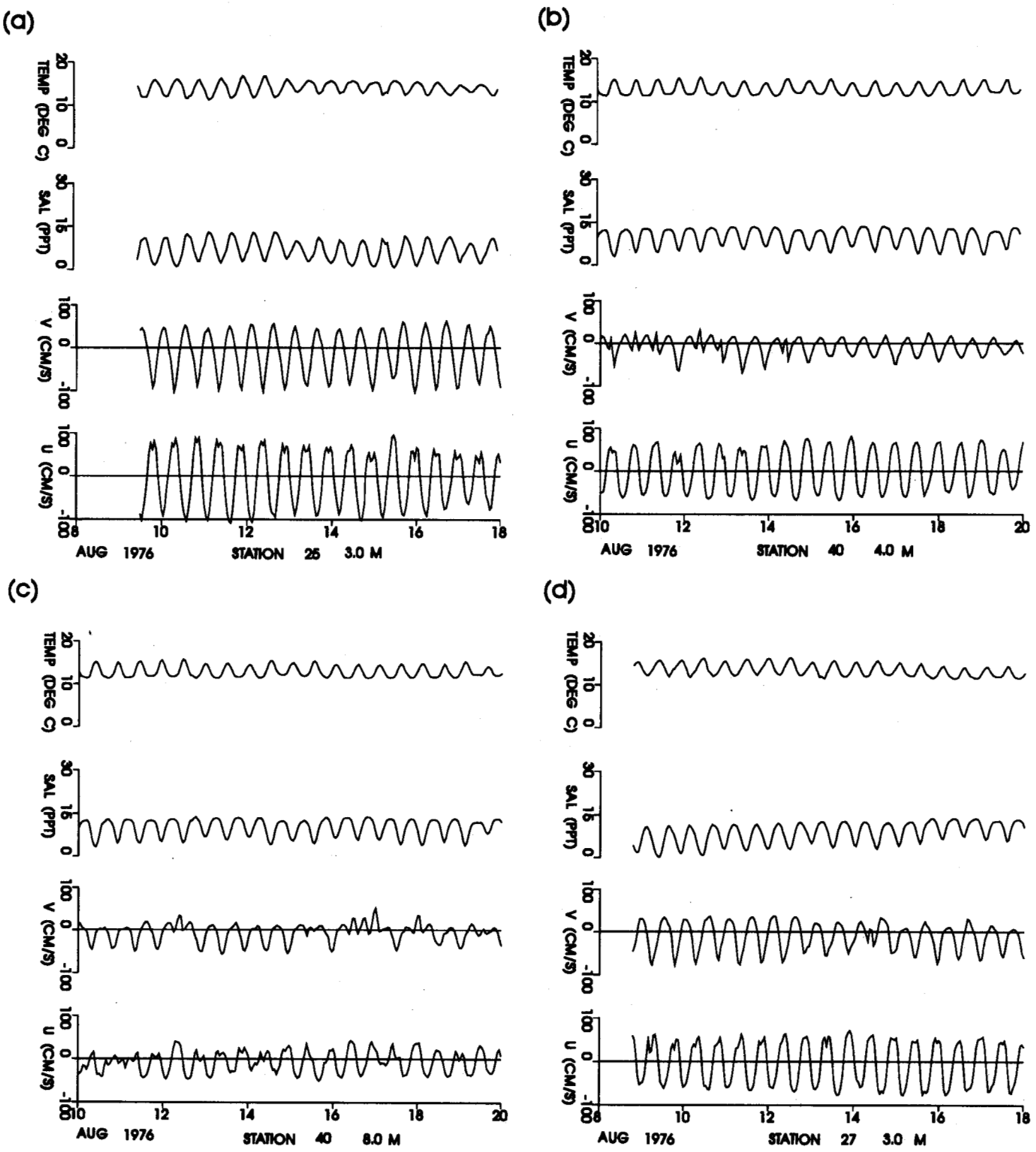


FIG. 9. Current meter data from transect A for August 1976: a) station 25 at 3.0 m; b) station 40 at 4.0 m; c) station 40 at 8.0 m; d) station 27 at 3.0 m.

velocity); and wind stress. Although Dyer (1977) pointed out that wind stress is potentially the most significant term in the lateral equation of motion, we could not confirm this because the dominant winds were mainly longitudinal, and strong tidal flows and bottom topography restrained cross-sectional wind-induced circulation. The wind stress was excluded from the examination. Estimation of the four remaining terms was made over the same ten consecutive semi-diurnal tidal cycles (11/08/76 at 11 h to 16/08/76 at 16 h) from the current meter data at the stations of transect A. Pressure measurements were adjusted hydrostatically to 3 m, and we used an average water density of 1006 $kg \cdot m^{-3}$. Table 5 lists the results of the analysis. The dominant terms in the lateral dynamic balance were found to be the centrifugal acceleration, the Coriolis force, and the baroclinic pressure gradient. The prominence of the centrifugal force was expected due to the strong tidal flow in this region

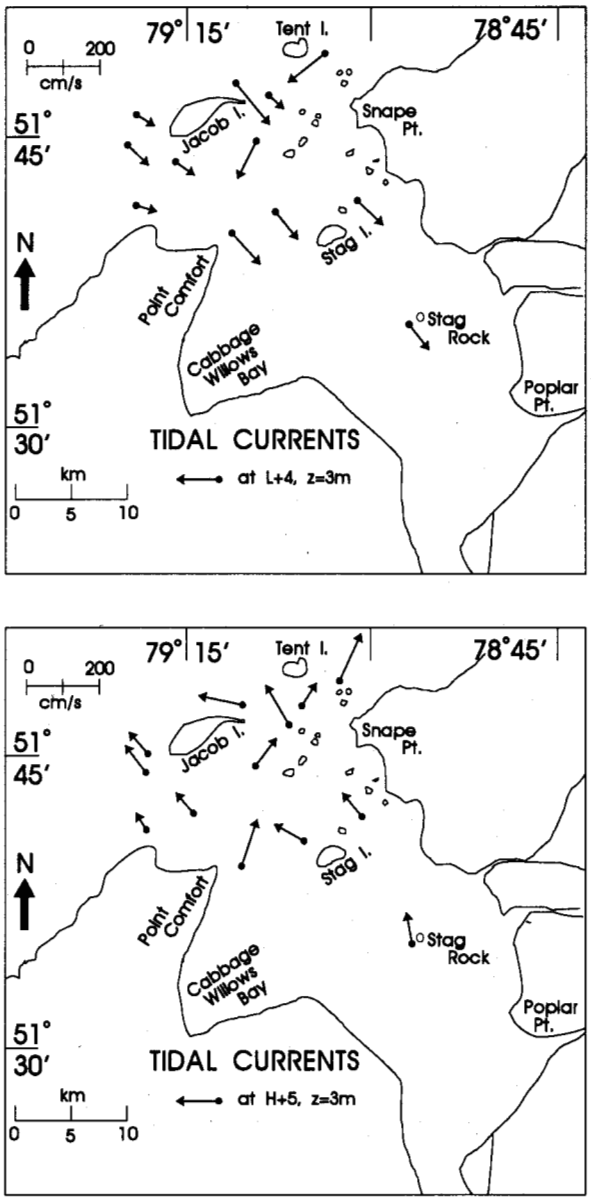


FIG. 10. a) Flood circulation (L+4) at z = 3 m and ebb circulation (H+5) at z = 3 m. b) Interpolated/extrapolated streamlines for H+5.

(up to 100 cm·s$^{-1}$ at station 25) and aerial observation. This term was twice as large as the Coriolis force. Figure 3 shows that the estuary is not laterally homogeneous at slack water. The baroclinic pressure gradient resulting from lateral density differences appeared strongest between stations 25 and 40. The residual contribution in Table 5 represents the contribution from the rate of change of the lateral velocity ($\frac{\partial \bar{v}}{\partial t}$), the other local accelerations, the horizontal pressure force resulting from the surface slope across the estuary, the turbulent Reynolds stresses, and, potentially, the excluded wind stress. Although the residual is of the same order as the Coriolis force, the contribution of the individual components is less than any of the forces balancing the acceleration ($\bar{v}\,\frac{\partial \bar{v}}{\partial y}$).

The main characteristics of the circulation in Rupert Bay were: 1) strong tidal currents compared to mean flow; 2) residual circulation controlled by the principal channels; 3) tidal currents using different paths at flood and ebb; 4) tidal current magnitudes that were about 30% lower at flood than at ebb; 5) surface currents that were much affected by wind stress along the main axis of the bay; and 6) secondary flows.

*Fronts*

The frontal zone is the area where large gradients in physical properties occur. The front itself is the line of demarcation in the frontal zone and is manifest at the surface by accumulations of foam or flotsam, similar to regions of convergence found in the open ocean, and by changes in water colouration due to gradients in sediment or plankton concentration. Fedorov (1983) provides a comprehensive discussion on defining fronts and semantics of related terms. According to him, two types of fronts can be associated with estuaries: that of a salt wedge, and that formed by interactions of tidal currents with bottom topography.

In Rupert Bay, fronts were similar to the tidal mixing fronts described by Simpson and Hunter (1974) and again by Fedorov. They were mostly aligned parallel to the axes of the main channels or around the downstream islands. Figure 11a depicts their approximate distribution derived from aerial pictures and visual observations. Since the fronts were observed to be present at various stages of the tide, the duration of the formations was presumed to be that of a tidal cycle. Their presence was also detectable on some of the current meter records, with a quick change of both transverse current velocity and of the salinity and temperature fields at maximum ebb.

TABLE 5. Lateral dynamic balance in Rupert Bay at transect A from hourly smoothed velocity and density measurements at stations 25, 27, and 40 where table units are $10^{-6}$ m·s$^{-2}$

$$\bar{v}\,\frac{\partial \bar{v}}{\partial y} = -\overline{\frac{1}{\rho}\frac{\partial P}{\partial y}} - f\bar{u} - \frac{\overline{u^2} + \overline{u}^2}{R}$$

| | Between stations 25 and 40 | Between stations 40 and 27 | Entire transect |
|---|---|---|---|
| $\bar{v}\,\frac{\partial \bar{v}}{\partial y}$ | −1.83 | 0.58 | −0.27 |
| $-\overline{\frac{1}{\rho}\frac{\partial P}{\partial y}}$ | 16.70 | −2.40 | 4.72 |
| $-f\bar{u}$ | 6.78 | 5.65 | 5.65 |
| $-\frac{\overline{u^2} + \overline{U}^2}{R}$ | −16.10 | −10.51 | −18.33 |
| Residual contribution | 5.55 | −6.68 | −8.23 |

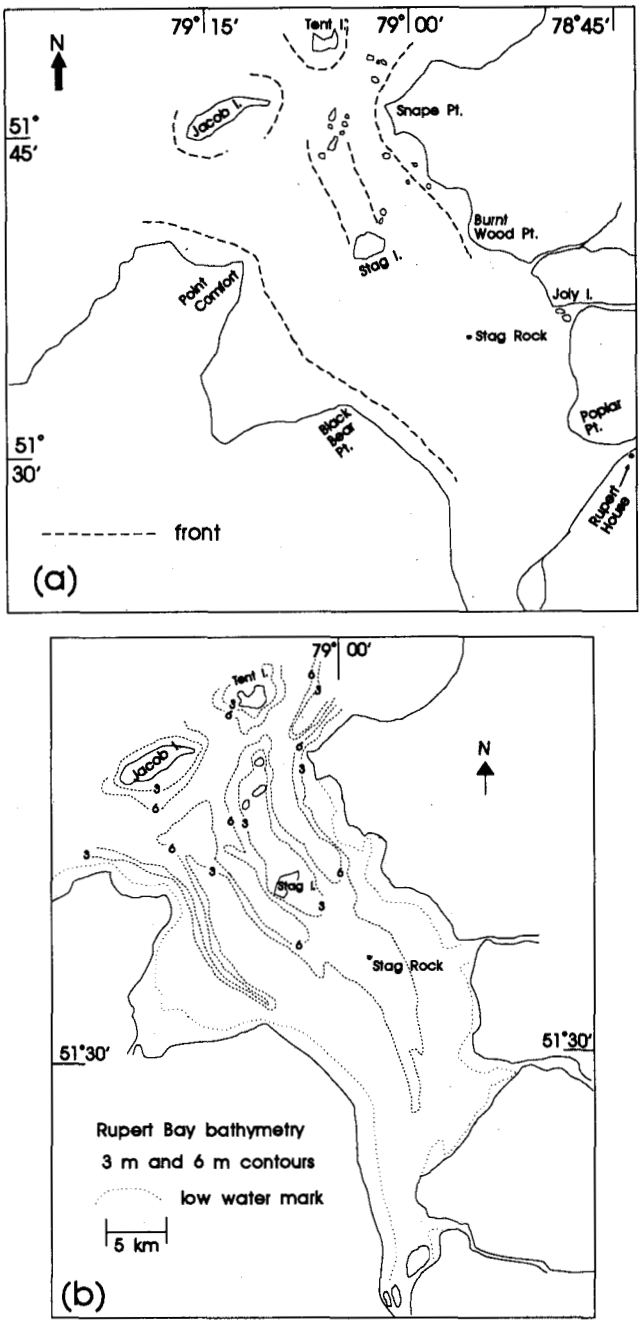


FIG. 11. a) Approximate frontal distribution derived from aerial photos and visual observations. b) Rupert Bay bathymetry.

Frontogenesis in Rupert Bay was thought to have occurred as a result of differential mixing caused by strong tidal flow over shoaling bottom topography, which created lateral gradients of density (Fig. 11b). Similar frontal formation was found by Huzzey (1988) and Huzzey and Brubaker (1988) for the York River estuary, a coastal plain estuary in Chesapeake Bay.

Simpson and Hunter (1974) developed an empirical model to predict frontal position in the Irish Sea according to local tidal currents and bathymetry. They suggested that the energy required to mix the water column was proportional to local depth ($h$) and to tidal energy loss. Since the tidal energy dissipation is proportional to the cube of tidal current intensity ($U^3$), they predicted frontal formation for $h/U^3 \approx 55$ (Simpson and Hunter, 1974). For tidal currents of 0.5 $m \cdot s^{-1}$, frontal formation should occur at about 7 m, while tidal currents of 1.0 $m \cdot s^{-1}$ would correspond to 55 m depth. Simpson and Hunter's criterion assumes that the tidal velocity at the bottom is proportional to the velocity at the surface and therefore uses the magnitude of the surface tidal velocity, whereas Pingree and Griffiths (1978) developed a variation of the above formula that had the advantage of using a a vertically averaged velocity. Since we observed little vertical velocity variation and shear in the water column, due probably to the shallowness of the study area, we used the Simpson and Hunter model to predict frontal formation. Tidal currents in the deeper channels of Rupert Bay were usually between 0.5 and 1.0 $m \cdot s^{-1}$, and since tidal currents were usually higher in the adjacent shallow areas, we expected all areas in Rupert Bay with depths less than 6 m to be homogeneous over most of the tidal cycle. An examination of Figures 6 and 11 confirms this hypothesis.

Biological implications of fronts and frontal zones can be characterized by the availability of nutrients and the amount of biomass. The front can act as a barrier for species and nutrients making one side high in productivity and the other much lower, with minimal mixing between the two water masses (Côté *et al.*, 1986; Simpson and Hunter, 1974). The biology of the observed frontal zones in Rupert Bay has never been specifically addressed and may be a topic worth further examination.

## CONCLUSION

Rupert Bay estuary is characterized by its shallow topography, strong tidal flow, and numerous fronts. Mixing was intense in the first two-thirds of its length, which created homogeneous conditions in many areas. Analysis of observed water level and current velocity confirmed the strong semidiurnal character of the tide and the presence of important shallow water constituents. Most of the observed non-tidal water level variations were well correlated with wind forcing. In-depth investigation of other phenomena occurring at tidal periods and non-tidal forcing, such as seiche and wind effects, may give further insight into mixing mechanisms in Rupert Bay. The cross-channel components of the flow were pertinent to the overall flow regime. An examination of the lateral dynamic balance at a mid-bay transect revealed that the centrifugal force, Coriolis force, and baroclinic pressure gradient between the southshore and mid-bay stations were the most significant of all estimated forces.

## ACKNOWLEDGEMENTS

The authors would like to thank Jean-Claude Deguise for his work in collecting the data. This work was supported by research grants from SEBJ and Hydro-Québec to GIROQ and by an NSERC operating grant to R.G. Ingram.

## REFERENCES

AUBREY, D.G., and SPEER, P.E. 1985. A study of non-linear tidal propagation in shallow inlet/estuarine systems. Part I: Observations. Estuarine, Coastal, and Shelf Science 21:185-205.

CÔTÉ, B., EL-SABH, M., and de la DURANTAYE, R. 1986. Biological and physical characteristics of a frontal region associated with the arrival of spring freshwater discharge in the southwestern Gulf of St. Lawrence. In: Skreslet, S., ed. The role of freshwater outflow in coastal marine ecosystems. NATO ASI Series, Vol. G7. Berlin: Springer-Verlag. 261-269.

d'ANGLEJAN, B. 1980. Effects of seasonal changes on the sedimentary regime of a subarctic estuary, Rupert Bay (Canada). Sedimentary Geology 26:51-68.

DEFANT, A. 1960. Physical oceanography. Vol. 2. London: Pergamon Press.

DUNBAR, M.J. 1982. Oceanographic research in Hudson and James bays. Naturaliste Canadien 109:677-683.

DYER, K.R. 1973. Estuaries: A physical introduction. Toronto: J. Wiley and Sons.

_____. 1977. Lateral circulation effects in estuaries. In: Estuaries, geophysics, and the environment. Washington, D.C.: National Academy of Sciences. 22-29.

FEDOROV, K.N. 1983. The physical nature and structure of oceanic fronts. Lecture notes on coastal and estuarine studies, No. 19. New York: Springer-Verlag.

FOREMAN, M.G.G. 1977. Manual for tidal heights analysis and prediction. Pacific Marine Science Report 77-10. Patricia Bay, Victoria, B.C.: Institute of Marine Sciences.

_____. 1978. Manual for tidal currents analysis and prediction. Pacific Marine Science Report 78-6. Patricia Bay, Victoria, B.C.: Institute of Marine Sciences.

FORRESTER, W.D. 1983. Canadian tidal manual. Ottawa: Department of Fisheries and Oceans, Canadian Hydrographic Service.

GODIN, G. 1972. The analysis of tides. Toronto: University of Toronto Press.

HANSEN, D.V., and RATTRAY, M. 1965. Gravitational circulation in straits and estuaries. Journal of Marine Research 23:104-122.

HUZZEY, L.M. 1988. The lateral density distribution in a partially mixed estuary. Estuarine, Coastal and Shelf Science 9:351-358.

HUZZEY, L.M., and BRUBAKER, J.M. 1988. The formation of longitudinal fronts in a coastal plain estuary. Journal of Geophysical Research 93: 1329-1334.

INGRAM, R.G., and CHU, V.H. 1987. Flow around islands in Rupert Bay: An investigation of the bottom friction effect. Journal of Geophysical Research 92:14521-14533.

KJERFVE, B. 1975. Velocity averaging in estuaries characterized by a large tidal range to depth ratio. Estuarine and Coastal Marine Science 3:311-323.

_____. 1986. Circulation and salt flux in a well mixed estuary. In: v. d. Kreeke, J., ed. Physics of shallow estuaries and bays. New York: Springer-Verlag. 22-29.

LEGENDRE, L., and SIMARD, Y. 1978. Dynamique estivale du phytoplancton dans l'estuaire de la Baie de Rupert (Baie de James). Naturaliste Canadien 105:243-258.

OFFICER, C.B. 1976. Physical oceanography of estuaries (and associated coastal waters). Toronto: J. Wiley and Sons.

PINGREE, R.D., and GRIFFITHS, D.K. 1978. Tidal fronts on the shelf seas around the British Isles. Journal of Geophysical Research 83:4615-4622.

PRINSENBERG, S.J. 1980. Man-made changes in the freshwater input rates of Hudson and James bays. Canadian Journal of Fisheries and Aquatic Sciences 37:1101-1110.

_____. 1982. Present and future circulation and salinity in James Bay. Naturaliste Canadien 109:821-841.

PRITCHARD, D.W. 1967. Observations of circulation in coastal plain estuaries. In: Lauff, G.H., ed. Washington, D.C.: American Association for the Advancement of Science. 37-44.

SEIM, H.E., and SNEED, J.E. 1988. Enhancement of semidiurnal tidal currents in the tidal inlets to Mississippi Sound. In: Aubrey, D.G., and Weishar, L., eds. Hydrodynamics and sediment dynamics of tidal inlets. New York: Springer-Verlag. 157-168.

SIMPSON, J., and HUNTER, J. 1974. Fronts in the Irish Sea. Nature 250: 404-406.

VEILLEUX, L. 1990. Physical oceanography of northern estuaries. M.Sc. thesis, McGill University, Montreal, Quebec, Canada.